Encapsulation and Covalent Binding of Molecular Payload in Enzymatically Activated Micellar Nanocarriers

Ido Rosenbaum,[†,§] Assaf J. Harnoy,[†,§] Einat Tirosh,[‡,§] Marina Buzhor,[†,§] Merav Segal,[†,§] Liat Frid,[†,§] Rona Shaharabani,[‡,§] Ram Avinery,[||,§] Roy Beck,[||,§] and Roey J. Amir*[,†,§]

[†]Department of Organic Chemistry, School of Chemistry, Faculty of Exact Sciences, [‡]Department of Physical Chemistry, School of Chemistry, Faculty of Exact Sciences, [§]Tel Aviv University Center for Nanoscience and Nanotechnology, and [||]School of Physics and Astronomy, Faculty of Exact Sciences, Tel-Aviv University, Tel-Aviv 69978, Israel

S *Supporting Information*

ABSTRACT: The high selectivity and often-observed over-expression of specific disease-associated enzymes make them extremely attractive for triggering the release of hydrophobic drug or probe molecules from stimuli-responsive micellar nanocarriers. Here we utilized highly modular amphiphilic polymeric hybrids, composed of a linear hydrophilic poly-ethylene glycol (PEG) and an esterase-responsive hydrophobic dendron, to prepare and study two diverse strategies for loading of enzyme-responsive micelles. In the first type of micelles, hydrophobic coumarin-derived dyes were encapsulated non-covalently inside the hydrophobic core of the micelle, which was composed of lipophilic enzyme-responsive dendrons. In the second type of micellar nanocarrier the hydrophobic molecular cargo was covalently linked to the end-groups of the dendron through enzyme-cleavable bonds. These amphiphilic hybrids self-assembled into micellar nanocarriers with their cargo covalently encapsulated within the hydrophobic core. Both types of micelles were highly responsive toward the activating enzyme and released their molecular cargo upon enzymatic stimulus. Importantly, while faster release was observed with noncovalent encapsulation, higher loading capacity and slower release rate were achieved with covalent encapsulation. Our results clearly indicate the great potential of enzyme-responsive micellar delivery platforms due to the ability to tune their payload capacities and release rates by adjusting the loading strategy.
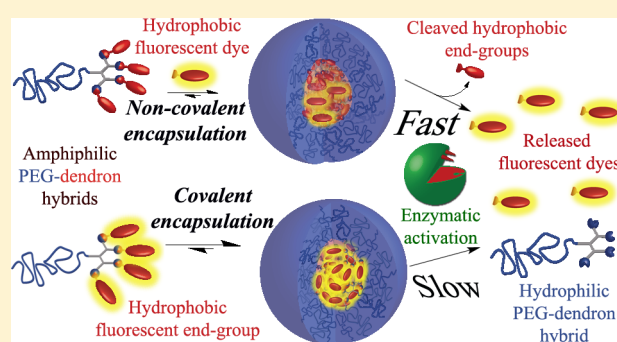
INTRODUCTION

Micellar nanocarriers composed of stimuli-responsive amphiphilic block copolymers are of interest due to their potential utilization in the field of controlled drug delivery.[1−4] Such smart micelles were shown to encapsulate hydrophobic molecular cargo (e.g., fluorescent dyes or drugs) within their hydrophobic cores and release them upon external stimuli that alter their amphiphilic nature.[5,6] Various types of stimuli-responsive polymers, which can switch their amphiphilic nature upon stimuli, have been reported to respond to irradiated light,[7−9] reduction,[10,11] changes in temperature[12−14] and pH,[15,16] or their combinations.[17−19] Enzymatic responsive block copolymers possess several significant advantages over polymers that respond to other stimuli for biomedical applications.[20−24] The catalytic nature, often-observed over-expression, and activity of specific disease-associated enzymes make them extremely attractive for selectively triggering the release of hydrophobic drug or probe molecules from such smart micellar nanocarriers. Yet, to date, there have been few reports on synthetic amphiphilic block copolymers that can self-assemble into stimuli-responsive micelles and disassemble upon enzymatic stimuli.[25−28]

We have recently reported on enzyme-responsive amphiphilic block copolymers composed of a hydrophilic poly-ethylene glycol (PEG) block and a dendron with enzymatically cleavable lipophilic end-groups as the hydrophobic block.[29] Cleavage of the hydrophobic end-groups by penicillin G amidase revealed primary amines that were protonated under physiological pH. This enzymatically induced decrease in amphiphilicity of the PEG-dendron hybrids results in destabilization and disassembly of the micelles and release of encapsulated Nile red molecules. Here, we demonstrate the modularity of these hybrids systems by introducing esterase cleavable end-groups and utilize this enzyme-responsive platform to study two distinct types of esterase-responsive carriers: noncovalently and covalently encapsulating micelles. A schematic representation of these two diverse loading strategies is presented in Figure 1.

In the first type of micelles, the hydrophobic guests are noncovalently encapsulated within the hydrophobic cores of the micelles. Enzymatic cleavage of the hydrophobic end-groups from the dendrons will lead to the formation of
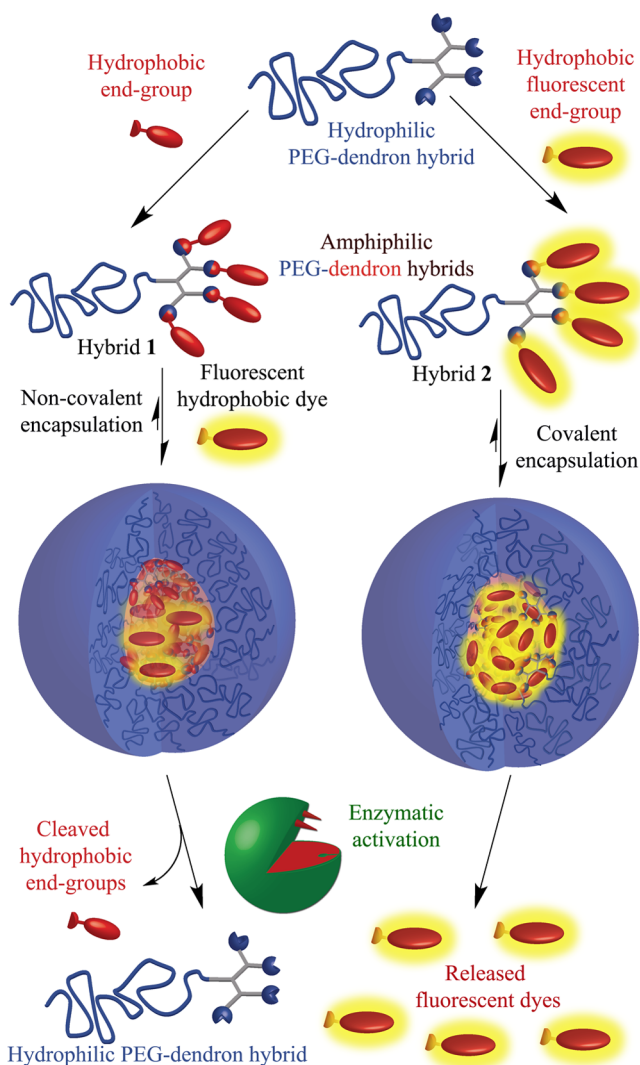
Figure 1. Schematic representation of noncovalent and covalent encapsulation of hydrophobic molecules in micellar nanocarriers.

hydrophilic PEG-dendron hybrids and result in disassembly of the micelles and subsequent release of the encapsulated molecules. In the second type of micelles, the hydrophobic molecular payload is covalently attached to the end-groups of the dendron block through enzymatically cleavable linkages. These covalently functionalized amphiphilic PEG-dendron hybrids are expected to self-assemble into micellar nanocarriers that covalently encapsulate their molecular cargo. In this case, the enzymatic cleavage of the hydrophobic end-groups would lead directly to the release of the "active" end-groups and simultaneously to the switching of the amphiphilicity of the hybrids as they become hydrophilic. Preliminary comparison of the loading capacities, stabilities, and release rates of these two diverse loading approaches demonstrates their potential application for drug delivery, revealing interesting insights into the unique features and challenges associated with each of these two loading strategies.

■ MOLECULAR DESIGN

To allow the direct comparison between the two loading approaches, we used 7-diethylamino-3-carboxycoumarin (coumarin acid) and its alkyl ester derivatives as model cargo molecules. Adjusting the length of the alkyl chains should

enable fine-tuning of the hydrophobicity of the dyes, which is a crucial parameter for noncovalent encapsulation. Furthermore, the carboxylic acid moiety can be used for conjugation to the dendron through an ester bond in order to allow its covalent encapsulation. Taking advantage of the modularity of our molecular design, we prepared two PEG-dendron hybrids, **1** and **2**, containing either four nonfluorescent phenyl acetate or four fluorescent coumarin-derived end-groups, respectively (Scheme 1). Hybrid **1** is expected to self-assemble into micelles

Scheme 1. Structures of PEG-Dendron Hybrids 1 and 2

PEG-dendron-(COCH$_2$Ph)$_4$
Hybrid **1**

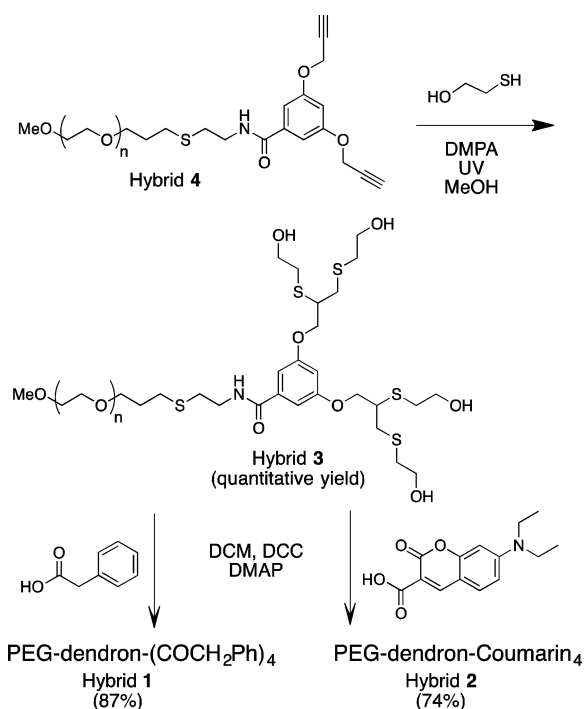PEG-dendron-Coumarin$_4$
Hybrid **2**
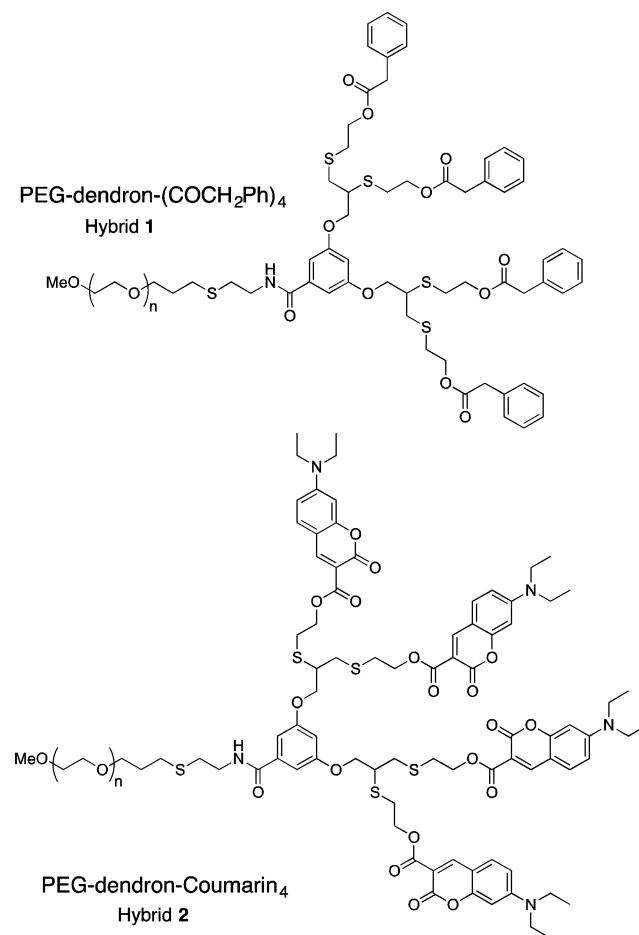
that will noncovalently encapsulate dye molecules, whereas hybrid **2** is expected to self-assemble into micellar nanocarriers that covalently bind the cargo molecules in their cores.

■ RESULTS AND DISCUSSION

Both amphiphilic hybrids were based on the hydrophilic tetra-hydroxy PEG-dendron, hybrid **3**, as a synthetic precursor (Scheme 2). Hybrid **3** is also the expected polymeric product after full enzymatic cleavage of the hydrophobic end-groups of hybrids **1** and **2**. Hybrid **3** was synthesized by thiol−yne reaction[30−32] of PEG-diyne (hybrid **4**)[29] with 2-mercaptoethanol to give hybrid **3** with four hydroxyl end-groups (Scheme 2). The hydrophilic precursor, hybrid **3**, was then functionalized with either phenyl acetic acid or 3-carboxy-7-diethylamino-coumarin to yield amphiphilic hybrids **1** and **2**, respectively. Hybrids **1**, **2**, and **3** were fully characterized by ^{1}H- and ^{13}C NMR, GPC, IR, and MALDI in order to confirm their structures, and the obtained experimental values are in good

Scheme 2. Synthesis of Esterase-Responsive Amphiphilic PEG-Dendron Hybrids
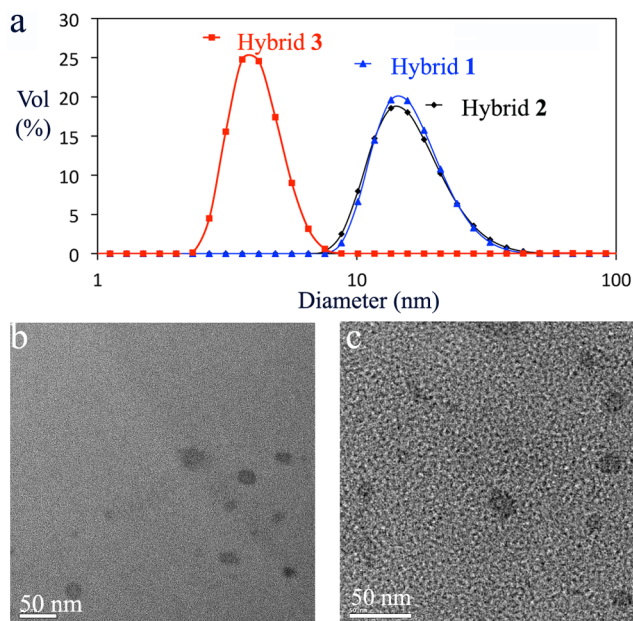

Figure 2. (a) DLS data of hydrophilic hybrid **3** and micelles formed by hybrids **1** and **2**. TEM images of micelles of (b) hybrid **1** and (c) hybrid **2**.

agreement with the theoretical ones (see Supporting Information).

The ability of amphiphilic hybrids **1** and **2** to self-assemble into micelles was first evaluated by dissolving them directly in aqueous buffer (phosphate buffer, pH 7.4) containing the solvatochromic dye Nile red.[33] Fluorescence measurements indicated comparable critical micelle concentrations (CMCs) of 3 ± 1 and 4 ± 1 μM for hybrids **1** and **2**, respectively. The sizes of the self-assembled structures were then characterized by dynamic light scattering (DLS) which indicated the formation of spherical nanostructures with diameters of 17 ± 5 nm (PDI 0.10) and 17 ± 6 nm (PDI 0.12) for hybrids **1** and **2**, respectively (Figure 2a). DLS measurements of hybrid **3** showed a diameter of 4 ± 1 nm (PDI 0.05), indicating its solubility and that it is in its monomeric form. Transmission electron microscopy (TEM) also validated the formation of spherical structures (Figure 2b,c). Further support for the formation of micelles with a PEG-shell and dendron-based core was obtained from ^{1}H NMR spectra of the PEG-dendron hybrids in D_2O (Figures S16A and S17A), which showed almost complete disappearance of the peaks corresponding to dendron protons; the peak corresponding to PEG protons remained unchanged when spectra in D_2O and $CDCl_3$ were compared.

After the self-assembly of the two PEG-dendron hybrids **1** and **2** into micelles was confirmed, their responses to enzymatic stimuli were studied using HPLC, fluorescence spectroscopy, DLS, and ^{1}H NMR. First, to gain an insight into the molecular mechanism of the enzymatic activation, we used HPLC to monitor the degradation of hybrids **1** and **2** by porcine liver esterase (PLE). Incubation with PLE resulted in cleavage of the end-groups and release of the hydrophilic hybrid **3** with almost no accumulation of partially cleaved hybrids (Figure 3); this is in contrast to our previously reported amidase-responsive micelles[29] that showed a significant accumulation of partially

cleaved amphiphilic hybrids. Although both hybrids **1** and **2** were fully degraded, the reaction rates were substantially different. Complete degradation of hybrid **1** was obtained in about 2.5 h in the presence of 0.23 μM PLE and in <30 min in the presence of 2.3 μM PLE (Figure 3c). In contrast, full cleavage of the coumarin esters in the presence of a 0.23 or 2.3 μM PLE was achieved only after 160 or 30 h, respectively (Figure 3c). These rate differences may be due to substrate specificity of the activating enzyme. To examine this hypothesis, we synthesized two low molecular weight ethyl esters: an ethyl 2-phenyl acetate and an ethyl-coumarin ester, **5a**. A mixture of both compounds was treated with PLE to enable evaluation of relative cleavage rates. The results clearly showed that the ethyl 2-phenyl acetate is a significantly better substrate, as its hydrolysis was much faster in comparison with that of the coumarin derivative (Figure S23). To further evaluate the stability of hybrids **1** and **2**, both hybrids were incubated in acidic buffer (pH 5.5), which represents acidic physiologic environments (e.g., endosomal pH).[34] Both hybrids were found to be completely stable under these conditions (Figures S26 and S27).

Next, DLS was used to confirm the disassembly of the micelles after enzymatic activation. Analysis before and after incubation with the activating enzyme, PLE, indicated the enzymatically triggered disassembly of the micelles as the peaks of the larger micellar aggregates disappeared and new peaks of smaller sizes appeared (Figure 4). These new peaks indicated the presence of structures with slightly larger diameters: 6 ± 3 nm (PDI 0.29) for hybrid **1** and 8 ± 3 nm (PDI 0.11) for hybrid **2**, than the expected diameters based on analysis of hybrid **3** (4 ± 1 nm). We assumed that the larger diameters result from the presence of the enzyme itself as it was measured to have a diameter of 8 ± 3 nm (PDI 0.17, Figure S15). To confirm this, we analyzed solutions of hybrid **3** with equivalent concentrations of the enzyme and were encouraged to see that the obtained DLS results for these mixtures of hybrid **3** and PLE were in good agreement with the sizes and size
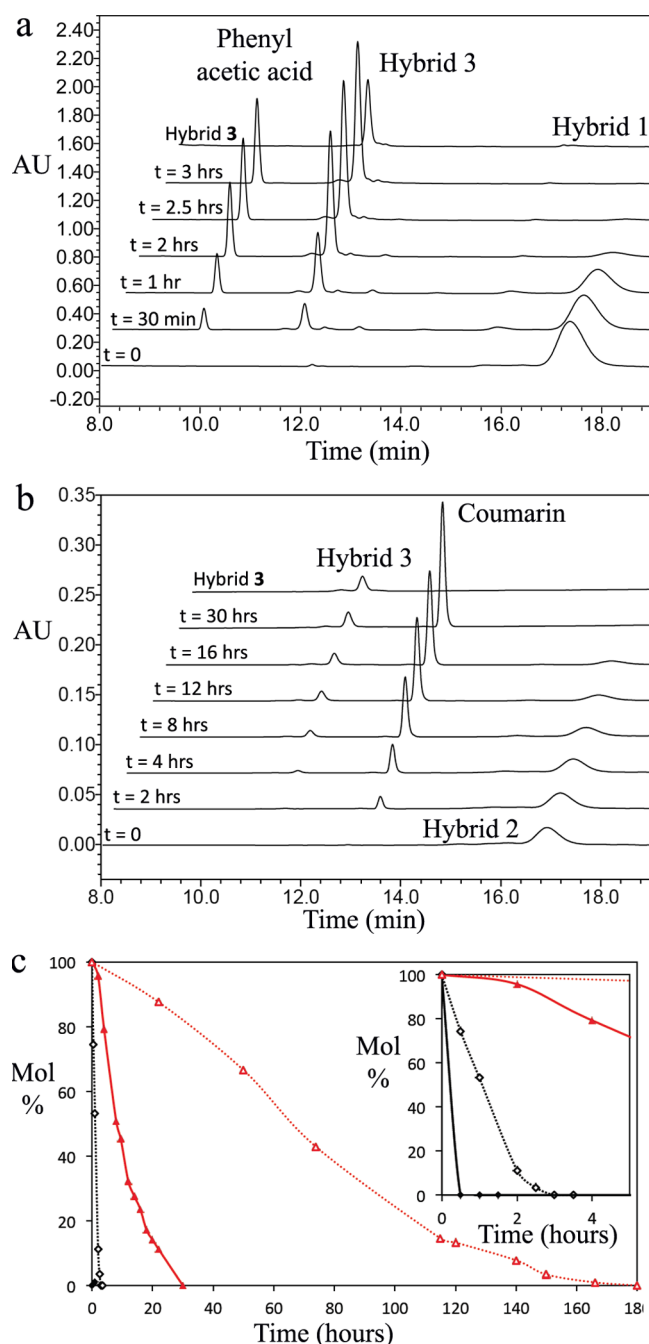
Figure 3. Overlays of HPLC chromatograms show almost direct transformation of (a) hybrid **1** (160 μM) into hydrophilic hybrid **3** in the presence of PLE (0.23 μM), measured at 215 nm and (b) hybrid **2** (160 μM) into hybrid **3** and the release of coumarin acid in the presence of PLE (2.3 μM), measured at 295 nm. (c) HPLC analysis of the degradation of hybrids **1** (black diamonds) and **2** (red triangles) in the presence of 2.3 μM (solid lines) or 0.23 μM (dashed lines) PLE. A zoom-in of the first 5 h appears in the inset (hybrids concentration = 160 μM).

Figure 4. DLS data of (a) hybrid **1** and (b) hybrid **2** show the disappearance of the peaks of the micelles and the formation of smaller structures after incubation with the activating enzyme, PLE (2.5 and 48 h for hybrids **1** and **2**, respectively). Mixtures of hybrid 3 with PLE 0.23 or 2.3 μM were analyzed to confirm that the larger than expected diameters resulted from the presence of the enzyme.

distributions that were measured for hybrids **1** and **2** after the enzymatic activation (Figure 4). These results indicate that the larger sizes observed for both hybrids after incubation with the enzyme and the significant increase in PDI in the case of hybrid **1** are due to the presence of the enzyme in the solutions.

After we demonstrated that the amphiphilic PEG-dendron hybrids self-assembled into micelles that were disassembled
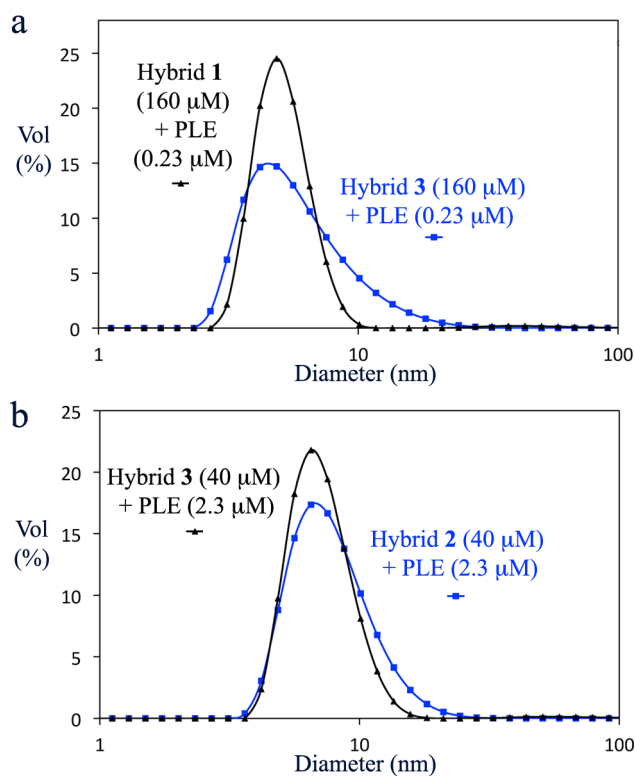
upon enzymatic triggering, we evaluated the correlation between the rate of enzymatic hydrolysis of hybrid **1** and the disassembly rate of the micelles. In order to measure the disassembly rate, we studied the release rate of encapsulated Nile red upon addition of the activating enzyme by using fluorescence spectroscopy. In the absence of the enzymatic stimulus, Nile red molecules are expected to be highly fluorescent as they are encapsulated within the hydrophobic cores of the micelles. Upon addition of the enzyme, a decrease in fluorescence is expected as Nile red molecules migrate from the disassembling hydrophobic cores of the micelles into the polar aqueous solution where its fluorescence is quenched. A decrease in fluorescence of the solution was observed as a function of time after addition of PLE (Figure 5a). An overlay of the HPLC degradation data and change in fluorescence as a function of time (Figure 5b) clearly shows excellent correlation between the rate of enzymatic hydrolysis of amphiphilic hybrid **1** and the decrease in fluorescence, indicative of the disassembly of the micelles and release of encapsulated Nile red.

Very interestingly, the fluorescence spectrum of amphiphilic hybrid **2** had maximum emission at 560 nm, which is significantly red-shifted—by nearly 90 nm—compared to the emission maxima of the coumarin acid or its ester derivatives at 470 nm. Since the binding of the dyes is not expected to change their electronic conjugation, this red shift must result from stacking of the bound dyes. To evaluate whether this stacking can occur at the monomer level and not only in the assembled micellar state, we measured the fluorescence of hybrid **2** at different concentrations above and below its CMC. As the red
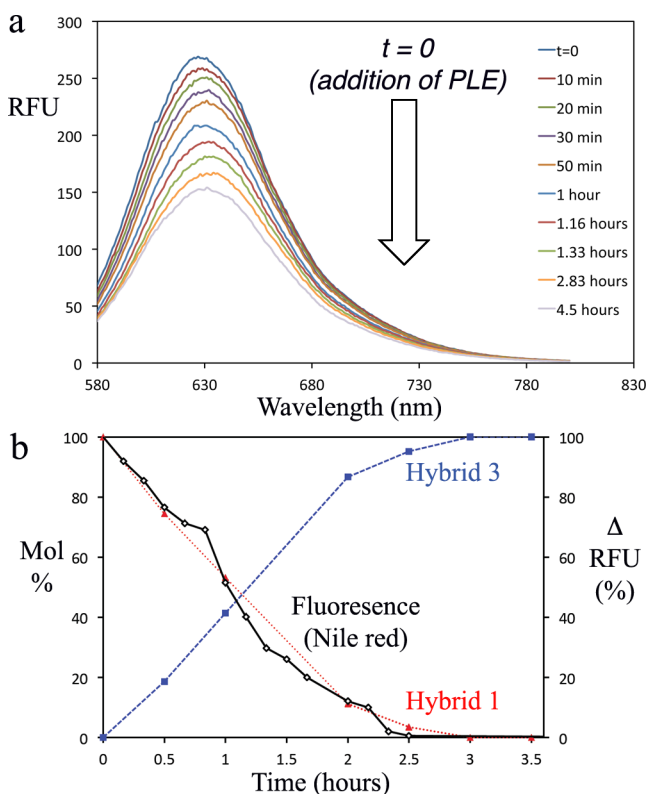
Figure 5. (a) Fluorescence spectra of encapsulated Nile red, indicating disassembly of the micelles and release of encapsulated dyes. (b) Overlay of the change in fluorescence intensity and HPLC analysis of the enzymatic degradation of hybrid **1**.

Figure 6. (a) Time-dependent fluorescence spectra of hybrid **2** (40 μM) after the addition of PLE (2.3 μM) show a decrease at 560 nm (hybrid **2**) and an increase at 470 nm (free coumarin). (b) Overlay of the changes in fluorescence (at 560 and 470 nm) and HPLC analysis of the enzymatic degradation of PEG-dendron hybrid **2**.

shift was observed at concentrations below the CMC of hybrid **2** (Figure S20), we concluded that it results from intramolecular stacking of the dyes within the monomeric hybrid. Fluorescence kinetic measurements showed that addition of PLE resulted in the decrease of emission at 560 nm and an increase at 470 nm, which is the expected emission wavelength for the released coumarin acid (Figure 6a). Overlay of the fluorescence and HPLC data indicates excellent correlation between the enzymatic degradation of amphiphilic hybrid **2** and the resulting change in fluorescence spectra (Figure 6b).

^{1}H NMR measurements further supported our hypothesis that the enzyme triggered disassembly of the micelles. As mentioned before, peaks of the protons of the hydrophobic dendron and end-groups are almost undetectable in ^{1}H NMR spectra in D$_2$O (Figures S16A and S17A). These peaks are present after incubation of the hybrids **1** and **2** with PLE (Figures S16D and S17D), indicating enzymatically induced disassembly of the hydrophobic core and formation of the hydrophilic hybrid **3**.

After the self-assembly and enzymatically triggered disassembly of both hybrids were well characterized, we utilized these two types of micelles to compare two diverse loading and release strategies: a classical noncovalent encapsulation and a covalent encapsulation approach. For covalent encapsulation, the loaded hydrophobic molecular cargo is covalently attached at the core of the micelle. To compare the two systems, we used polymer concentrations of 40 μM, which is well above the measured CMC values of around 3.5 μM. At this polymer concentration there is the potential for release of 160 μM coumarin dye from hybrid **2**. Hence, this coumarin concentration was also used for loading experiments of hybrid
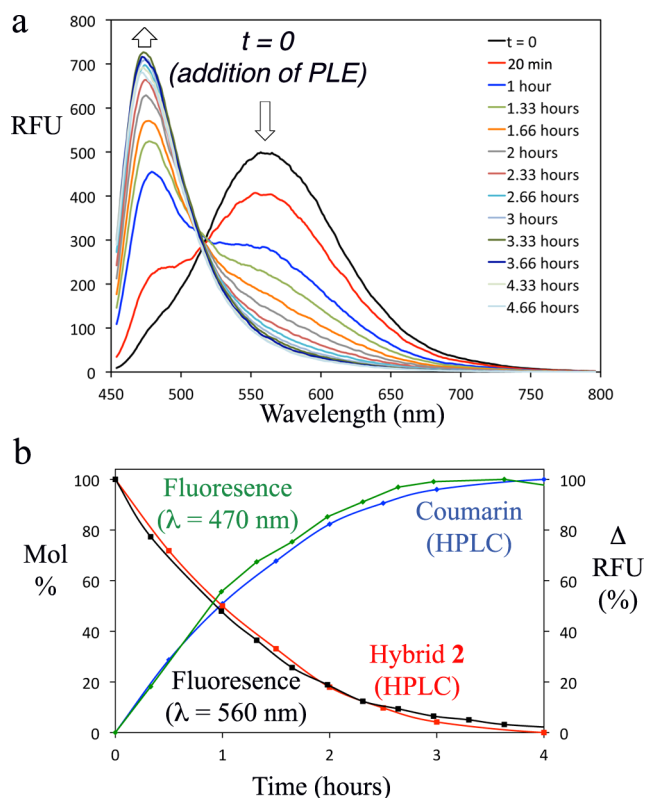
1. Due to the relative hydrophilicity of the coumarin acid, we decided to increase its hydrophobicity by preparing ester derivatives that could be hydrolyzed into the acid form by the same activating enzyme. As detailed below, the hydrophobicity of the encapsulated dyes was found to substantially affect the degree of their encapsulation.

Noncovalent loading of the micelles was done by preparing a concentrated stock solution of the dyes in DMSO and diluting this solution directly into an aqueous solution of amphiphilic hybrid **1** to yield the desired polymer and dye concentrations. The release experiments were carried out by placing a solution containing the loaded micelles into a dialysis tube with a molecular weight cutoff (MWCO) of a 1 kDa. This MWCO allows equilibration of the released coumarin dyes, while the high molecular weight PEG-dendron hybrids are retained. The amount of released dye was measured in the presence and absence of the activating enzyme by HPLC analysis of samples that were taken periodically from the solution outside of the dialysis tube. These experiments allowed us to evaluate the micellar encapsulation capacities by monitoring the background release in the absence of the activating enzyme and allowed us to determine the release kinetics from both types of micelles. The amount of released dye was compared to the amount of dye that was initially added to the micelles.

Measurements of background release (or leakage) of encapsulated dye from the micelles were first obtained for ethyl-coumarin ester **5a** (Figure 7a). The data showed that a significant amount of dye was released in the absence of enzyme (Figure 7b), resulting in a loading ratio of 1.1 coumarin molecules per PEG-dendron hybrid. This rather high leakage,
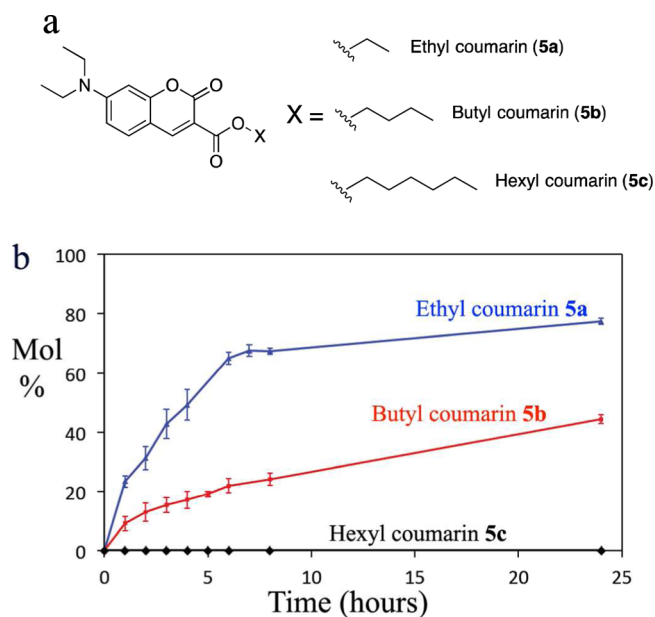
Figure 7. (a) Structures of coumarin derivatives **5a−c** and (b) HPLC analysis of background release of dyes from micelles based on hybrid **1** in the absence of the activating enzyme.

which indicates a relatively low encapsulation capacity, motivated us to prepare two more coumarin-ester derivatives, **5b** and **5c** (Figure 7a). These two dyes have higher hydrophobicities than **5a** due to replacement of the ethyl ester group of **5a** with butyl or hexyl chains, respectively (Figure 7a). Encapsulation and release experiments with the butyl derivative **5b** showed a significant decrease in the background leakage of the dye (Figure 7b) and an increase in the degree of encapsulation (2.2 dye molecules per polymer chain) relative to encapsulation of **5a**.

Although the direct dilution of concentrated stock solutions of both ethyl- and butyl-coumarin derivatives, **5a** and **5b**, into buffer solutions that contained micelles of hybrid **1** resulted in the formation of clear solutions, indicating full solubility of the dyes in the presence of the micelles, a different behavior was observed for the hexyl-coumarin derivative, **5c**. In this case, probably due to the higher hydrophobicity of the dye, some precipitation occurred. This solution was filtered to remove any nonsoluble aggregates. Analysis of the filtrate by HPLC revealed that the effective concentration of the hexyl-coumarin derivate **5c** was decreased to around 30 μM, which translates to encapsulation capacity of about 0.75 dye molecule per polymer chain. Interestingly, when the loaded micelles were analyzed in the dialysis experiment, no leakage of dyes was observed in the absence of the enzyme (Figure 7b). The stability of the complex with **5c** is most likely due to the high hydrophobicity and extremely low aqueous solubility of the hexyl-derivatized dye.

Next, release of dyes **5a−c** from micelles based on hybrid **1** in the presence of the activating enzyme PLE (0.23 μM) was evaluated. It is important to note that the encapsulated dyes contained ester functionalities, which could also be hydrolyzed by the enzyme to give the free coumarin acid. Hence, the total amounts of both coumarin acid and coumarin esters were taken into account when evaluating the amounts of released dyes. To our delight, nearly full release of the encapsulated dyes was observed for all three coumarin derivatives **5a−c**, and the release rates were similar for the three dyes regardless of their

hydrophobicity (Figure 8). These results demonstrate that release of a variety of encapsulated molecules from these smart micellar nanocontainers is triggered specifically by enzymatic activation.
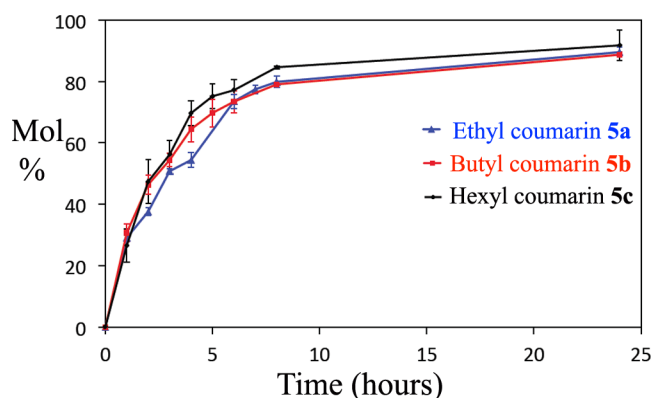

Figure 8. HPLC analysis of the combined release of coumarin derivatives, **5a−c**, and free coumarin acid from micelles based on hybrid **1** in the presence of 0.23 μM activating enzyme PLE.

To further evaluate the enzymatic control over the release rate, micelles based on hybrid **1** and loaded with butyl-coumarin **5b**, were incubated in the presence of lower concentrations of the activating enzyme PLE (69, 23, and 7.7 nM). Slower release rates were observed for the two lower concentrations compared to the presence of a higher enzyme concentration (Figure 9). In the case of 69 nM of PLE, the
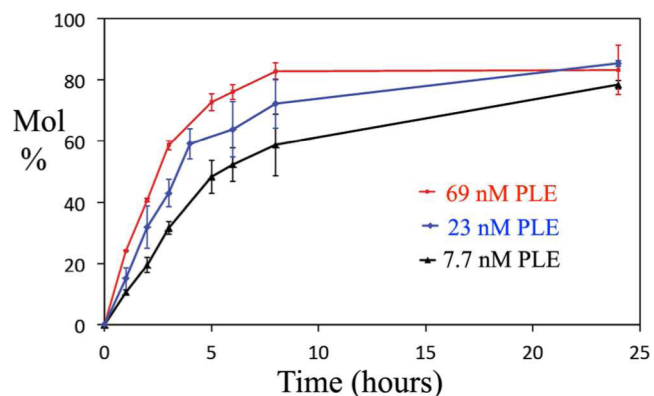

Figure 9. HPLC analysis of the combined release of butyl coumarin ester, **5b**, and free coumarin acid from micelles based on hybrid **1** in the presence of 69 nM (red), 23 nM (blue) and 7.7 nM (black) activating enzyme PLE.

release rate was similar to the rate observed for the release in the presence of 0.23 μM (Figure 8), as in this case the rate of release is probably influenced mostly by the rate of diffusion of the dye through the dialysis tube. These results show good correlation between the concentrations of the activating enzyme and the release rate of the hydrophobic molecular cargo from the micelles. Once the end-groups, which constitute the encapsulating hydrophobic cores, are enzymatically cleaved, the hybrids lose their amphiphilic nature, and the micelles fall apart to release their molecular cargo.

As mentioned before, dye molecules **5a−c** are esters of coumarin with hydrophobic aliphatic side chains that can be cleaved by the same enzyme that triggers their release from the

micelle. Hence we expected that these ester derivatives would be cleaved to release free coumarin acid in parallel with the enzymatic activation of the disassembly process. The release of coumarin acid can be viewed as a model of potential encapsulation and release of prodrugs, which can be transformed into the parent drug by the same enzyme that triggers the disassembly of the carrying micelles. This approach addresses one of the most important requirements of a drug delivery platform: The parent drug must be released, not a modified derivative that may be less active and that would require FDA approval. Very interestingly, analysis of the composition of dyes that was released from micelles of hybrid **1**, which were loaded with ethyl coumarin **5a** and placed in the dialysis tube, revealed that ~80−90% of the released dyes were coumarin acid due to the enzymatic hydrolysis of coumarin ester **5a**, yet a significant amount of coumarin ester (~10−20% of the initial amount of dyes that was loaded into the dialysis tube) was still observed (Figure 10a). This is in contrast to the
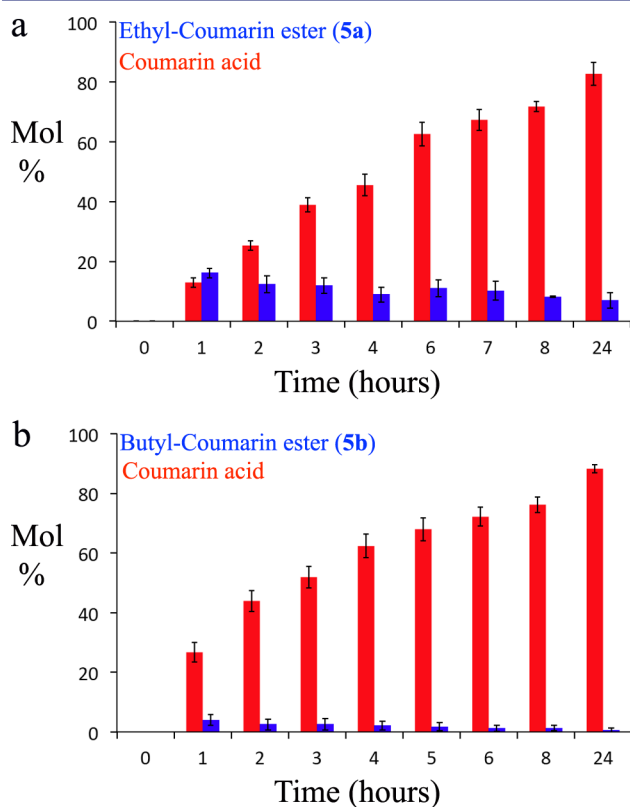

Figure 10. Comparison of the molar percentages (out of the initial amount of dyes that were loaded into the dialysis tube) of coumarin ester (blue) and coumarin acid (red) that were released from micelles based on hybrid **1** loaded with dyes (a) **5a** and (b) **5b** in the presence of 0.23 μM activating enzyme PLE.

compositions of dyes that were released from micelles loaded with the derivatives **5b** and **5c** bearing butyl and hexyl chains, respectively. In these cases, almost complete enzymatic hydrolysis of the esters was observed, and only low percentages (<5% of the initial amount of dyes that were loaded into the dialysis tube) of the unhydrolyzed esters **5b** and **5c** were detected (Figures 10b and S28, respectively).

In order to better understand these results we decided to carry out an additional experiment to evaluate the relative enzymatic hydrolysis rates of the three coumarin esters **5a−c**.

In this experiment, we co-encapsulated the three dyes (20 μM of each dye) in micelles based on hybrid **1** (40 μM) and evaluated their relative degradation in the presence of the activating enzyme by HPLC. The obtained HPLC data clearly indicated that butyl and hexyl coumarin esters were hydrolyzed more rapidly than was the ethyl derivative **5a** (Figure S24). These rate differences explain the higher amount of ethyl-ester **5a** that was released in our dialysis-based encapsulation and release experiments.

After the characterization of noncovalent encapsulation and enzymatically triggered release of hydrophobic dyes from micelles based on hybrid **1**, amphiphilic hybrid **2** was utilized to study the covalent encapsulation approach. The release experiments for covalently encapsulating micelles were carried out by directly dissolving a powder form of hybrid **2** into buffer solution to form the micelles. The release of the dye from the micelles in the presence and absence of the activating enzyme was studied using the dialysis setup described earlier for hybrid **1**. The first notable differences between the two loading approaches are the high control over the ratio of dyes per polymer and stability of the loaded micelle that could be achieved by covalent conjugation of the dye molecules to the dendron. This is in contrast to the noncovalent loading strategy, which strongly depends on the supramolecular interactions between the dyes and the hydrophobic cores and hence is more difficult to control or tune. Remarkably, although hybrid **2**-based micelles have a higher loading ratio (4 dyes per polymer chain) than the hybrid **1**-based micelles, no release of dyes was observed in the absence of the enzyme (Figure 11),
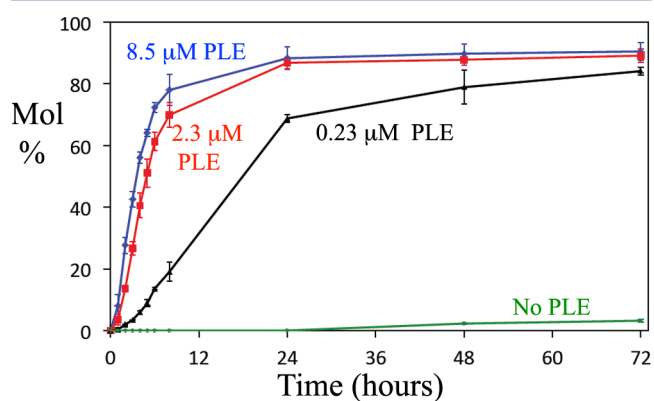

Figure 11. HPLC analysis of the release of coumarin acid from micelles based on hybrid **2** in the absence (green circles) and the presence of activating enzyme PLE: 0.23 μM (black triangles), 2.3 μM (red squares), and 8.5 μM (blue diamonds).

indicating the high stability of the loaded micelles. Another significant difference was that the enzymatic hydrolysis of the coumarin-based end-groups from hybrid **2** occurred more slowly than the cleavage of the phenyl acetic ester groups in hybrid **1** (Figure 3c). Based on this slower hydrolysis rate, we expected a slower release of dyes from micelles based on amphiphilic hybrid **2**. HPLC monitoring of the release showed that nearly full release was achieved from hybrid **2** micelles after almost 2 days in the presence of 0.23 μM PLE; in contrast, the noncovalently encapsulating micelles released their cargo in few hours under similar conditions. The release rate for the hybrid **2** micelles depended on the concentration of the activating enzyme, and increases of 10-fold (2.3 μM) in the concentrations of PLE resulted in nearly full release at

significantly shorter times (Figure 11). Further increase in the enzyme concentration to 8.5 μM resulted in a relatively small increase in release rate, indicating that at these relatively high enzyme concentrations, the diffusion rate through the dialysis tubes probably becomes the rate-limiting step in the release of the dyes.

The covalent-encapsulation approach offered higher stability and, most importantly, the potential for tuning the number of loaded cargo molecules by simply adjusting the generation of the dendron and its number of end-groups. This approach has some limitations: for example, the specificity of the activating enzyme may limit the variety of compounds that can be used. In some cases, the molecular cargo might not be cleavable at all due to structural differences from the natural substrate of the activating enzyme. In addition, specific functional groups are needed for the conjugation to the dendron. This is in contrast to the noncovalent encapsulation, which relies on less specific hydrophobic interactions and therefore can accommodate a greater variety of guest molecules. Furthermore, the release rate from the noncovalently encapsulating micelles depended on the rate of enzymatic hydrolysis of the "benign" hydrophobic end-groups and not on the hydrophobicity of the guest molecules.

CONCLUSIONS

Taking advantage of the high modularity of the PEG-dendron hybrids, we prepared two esterase-responsive amphiphilic PEG-dendrons through a very simple and efficient synthetic methodology. The enzyme cleavable end-groups were phenyl acetic or coumarin esters. Both hybrids had comparable CMC values and self-assembled into micelles with similar diameters. Utilizing the two hybrids we assembled noncovalently and covalently encapsulating micelles and carried out a comparison of their hydrolysis rates, encapsulation capacities, stabilities, and release rates. Both types of micelles were highly responsive toward the activating enzyme, and almost full release of the loaded molecular cargo was observed upon enzymatic stimulus. Importantly, the noncovalent encapsulation enables faster release rates and the use of a broader scope of molecules that can be encapsulated. On the other hand, higher loading capacity and slower release rates were achieved by covalent encapsulation. This range of release rates and the ability to tune them make this delivery platform relevant to various applications. Notably, noncovalently encapsulating micelles based on hybrid **1**, which were loaded with highly hydrophobic dye (hexyl coumarin **5c**), and covalently encapsulating micelles based on hybrid **2** were stable, and almost no release of dyes was observed in the absence of the activating enzyme.

The noncovalent encapsulation strongly depends on the specific properties of the encapsulated cargo and the nature of the micellar core and therefore is more difficult to tune. Nevertheless, in some cases, in which the molecular cargo lacks the proper functional groups, noncovalent encapsulation is the only possible loading strategy. In contrast, covalent binding of hydrophobic cargo molecules to the dendron resulted in higher loading capacity that potentially can be tuned by adjusting the generation and number of end-groups of the dendron. The obtained results clearly demonstrate the great potential of these modular, enzymatically activated delivery platforms due to the ability to tune their payload capacities and release rates by adjusting the loading strategy. Enzyme responsive nanocarrier micellar systems can be envisioned to allow in the future the selective release of active payload only in the presence of specific enzymes at the target site.

ASSOCIATED CONTENT

Ⓢ Supporting Information

Detailed experimental information, characterization data, CMC measurements, UV and fluorescence spectra, HPLC conditions and data, and encapsulation and release experiments. This material is available free of charge via the Internet at http://pubs.acs.org.

AUTHOR INFORMATION

Corresponding Author

*amirroey@tau.ac.il

Notes

The authors declare no competing financial interest.

ACKNOWLEDGMENTS

REFERENCES

(1) Mai, Y.; Eisenberg, A. *Chem. Soc. Rev.* **2012**, *41*, 5969.

(2) Kataoka, K.; Harada, A.; Nagasaki, Y. *Adv. Drug Delivery Rev.* **2012**, *37*, 48.

(3) Rösler, A.; Vandermeulen, G.; Klok, H.-A. *Adv. Drug Delivery Rev.* **2012**, *64*, 270.

(4) Roy, D.; Cambre, J. N.; Sumerlin, B. S. *Prog. Polym. Sci.* **2010**, *35*, 278.

(5) Cabane, E.; Zhang, X.; Langowska, K.; Palivan, C. G.; Meier, W. *Biointerphases* **2012**, *7*, 9.

(6) Zelzer, M.; Todd, S. J.; Hirst, A. R.; McDonald, T. O.; Ulijn, R. V. *Biomater. Sci.* **2013**, *1*, 11.

(7) Lee, H.-I.; Wu, W.; Oh, J. K.; Mueller, L.; Sherwood, G.; Peteanu, L.; Kowalewski, T.; Matyjaszewski, K. *Angew. Chem., Int. Ed.* **2007**, *46*, 2453.

(8) Muraoka, T.; Koh, C.-Y.; Cui, H.; Stupp, S. I. *Angew. Chem., Int. Ed.* **2009**, *48*, 5946.

(9) Yesilyurt, V.; Ramireddy, R.; Thayumanavan, S. *Angew. Chem., Int. Ed.* **2011**, *50*, 3038.

(10) Zhuang, Y. Y.; Su, Y.; Peng, Y.; Wang, D. L.; Deng, H. P.; Xi, X. D.; Zhu, X. Y.; Lu, Y. F. *Biomacromolecules* **2014**, *15*, 1408.

(11) Wang, L.; Cao, W.; Yi, Y.; Xu, H. *Langmuir* **2014**, *30*, 5628.

(12) Lee, H.; Lee, J.; Poon, Z.; Hammond, P. *Chem. Commun.* **2008**, 3726.

(13) Andre, X.; Zhang, M.; Mueller, A. *Macromol. Rapid Commun.* **2005**, *26*, 558.

(14) Fuller, J.; Raghupathi, K.; Ramireddy, R. R.; Subrahmanyam, A.; Yesilyurt, V.; Thayumanavan, S. *J. Am. Chem. Soc.* **2013**, *135*, 8947.

(15) Lundberg, P.; Lynd, N.; Zhang, Y.; Zeng, X.; Krogstad, D.; Paffen, T.; Malkoch, M.; Nyström, A.; Hawker, C. J. *Soft Matter* **2013**, *9*, 82.

(16) Gillies, E. R.; Jonsson, T. B.; Frechet, J. M. J. *J. Am. Chem. Soc.* **2004**, *126*, 11936.

(17) Loh, X.; del Barrio, J. S.; Toh, P.; Lee, T.-C.; Jiao, D.; Rauwald, U.; Appel, E.; Scherman, O. *Biomacromolecules* **2011**, *13*, 84.

(18) Zhang, Q.; Vanparijs, N.; Louage, B.; De Geest, B. G.; Hoogenboom, R. *Polym. Chem.* **2014**, *5*, 1140.

(19) Zhuang, J.; Chacko, R.; Amado Torres, D.; Wang, H.; Thayumanavan, S. *ACS Macro Lett.* **2014**, *3*, 1.

(20) Rao, J.; Hottinger, C.; Khan, A. *J. Am. Chem. Soc.* **2014**, *136*, 5872.

(21) Chien, M. P.; Carlini, A. S.; Hu, D.; Barback, C. V.; Rush, A. M.; Hall, D. J.; Galya Orr, G.; Nathan C. Gianneschi, N. C. *J. Am. Chem. Soc.* **2013**, *135*, 18710.

(22) Ku, T.-H.; Chien, M.-P.; Thompson, M. P.; Sinkovits, R. S.; Olson, N. H.; Baker, T. S.; Gianneschi, N. C. *J. Am. Chem. Soc.* **2011**, *133*, 8392.

(23) Amir, R. J.; Zhong, S.; Pochan, D. J.; Hawker, C. J. *J. Am. Chem. Soc.* **2009**, *131*, 13949.

(24) Rao, J.; Khan, A. *J. Am. Chem. Soc.* **2013**, *135*, 14056.

(25) Guo, J.; Zhuang, J.; Wang, F.; Raghupathi, K.; Thayumanavan, S. *J. Am. Chem. Soc.* **2014**, *136*, 2220.

(26) Samarajeewa, S.; Zentay, R. P.; Jhurry, N. D.; Ang, L.; Seetho, K.; Zou, J.; Wooley, K. L. *Chem. Commun.* **2014**, *50*, 968.

(27) Daniel Bacinello, D.; Garanger, E.; Taton, D.; Tam, K. C.; Lecommandoux, S. *Biomacromolecules* **2014**, *15*, 1882.

(28) Raghupathi, K.; Azagarsamy, M.; Thayumanavan, S. *Chem.—Eur. J.* **2011**, *17*, 11752.

(29) Harnoy, A. J.; Rosenbaum, I.; Tirosh, E.; Ebenstein, Y.; Shaharabani, R.; Beck, R.; Amir, R. J. *J. Am. Chem. Soc.* **2014**, *136*, 21.

(30) Fairbanks, B. D.; Sims, E. A.; Anseth, K. S.; Bowman, C. N. *Macromolecules* **2010**, *43*, 4113.

(31) Ghiradello, M.; Öberg, K.; Staderini, S.; Renaudet, N.; Dumy, P.; Hed, Y.; Marra, A.; Malkoch, M.; Dondoni, A. *J. Polym. Sci., Part A: Polym. Chem.* **2014**, *52*, 2422.

(32) Sharma, R.; Naresh, K.; Chabre, Y. M.; Rej, R.; Saadeh, N. K.; Roy, R. *Polym. Chem.* **2014**, *5*, 4321.

(33) Leenders, C. M. A.; Albertazzi, L.; Mes, T.; Koenigs, M. M. E.; Palmans, R. A.; Meijer, E. W. *Chem. Commun.* **2013**, *49*, 33.

(34) Sorkin, A.; Von Zastrow, M. *Nat. Rev. Cell. Biol.* **2002**, *3*, 600.